Open and Hidden Charm Production in 920 GeV Proton-Nucleus Collisions

U. Husemann[a] for the HERA-B Collaboration

[a]Fachbereich Physik, Universität Siegen, Walter-Flex-Str. 3, D–57068 Siegen, Germany

The HERA-B collaboration has studied the production of charmonium and open charm states in collisions of 920 GeV protons with wire targets of different materials. The acceptance of the HERA-B spectrometer covers negative values of x_F up to $x_F = -0.3$ and a broad range in transverse momentum from 0.0 to 4.8 GeV/c. The studies presented in this paper include J/ψ differential distributions and the suppression of J/ψ production in nuclear media. Furthermore, production cross sections and cross section ratios for open charm mesons are discussed.

1. Introduction

Studying charmonium and open charm hadroproduction provides a good test of the theoretical production models available and their modifications in nuclear media. Since many of these models rely on experimental data to adjust their free parameters, a comprehensive test of the model predictions in a broad kinematic range and with good precision is desirable.

HERA-B is in the position to extend previous measurements of J/ψ production and nuclear suppression to negative x_F values. D^0 and D^+ production cross sections and cross section ratios are determined with high accuracy.

2. The HERA-B Detector and Trigger

The HERA-B detector is a fixed-target spectrometer with large angular acceptance. The detector includes subdetectors for vertexing, tracking, and particle identification, as shown in Fig. 1.

Protons with energies of 920 GeV are brought into collisions with an internal wire target. The target consists of two stations of four wires each, separated by 4 cm along the beam axis. Each wire can be moved independently in the halo of the proton beam to adjust the interaction rate.

The vertex detector system (VDS) allows for reconstruction and separation of primary and secondary vertices. It consists of eight double-layers of double-sided silicon strip detectors. The tracking detector is divided into an inner part consisting of micro-strip gaseous chambers with gas electron multiplier foils and an outer part of honeycomb drift chambers.

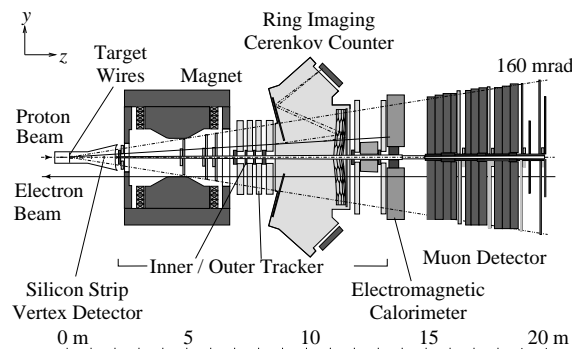The particle identification devices include a ring-

Figure 1. Side view of the HERA-B detector.

imaging Čerenkov counter (RICH), an electromagnetic calorimeter (ECAL), and a four-layer muon detector.

In HERA-B, a multilevel trigger system is employed to enrich lepton pairs from J/ψ decays. Pre-triggers in the muon detector and ECAL provide track seeds for the first level trigger (FLT). The FLT performs a track search in the outer tracker. In the second trigger level, the tracking of the FLT is confirmed, tracks are extrapolated to the VDS, and a vertex fit is performed for pairs of leptons. Accepted events are reconstructed online. Alternatively, a minimum bias trigger can be utilized, requiring either a minimum number of photons in the RICH or a minimum energy deposit in the ECAL.

3. The 2002/2003 Data-Taking Period

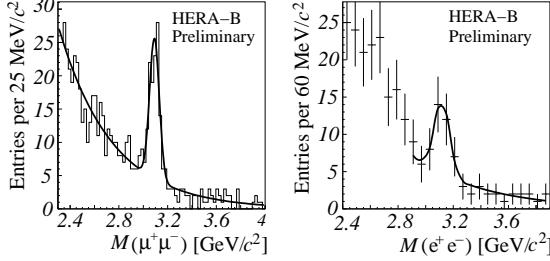The results presented in this paper are based on data taken with the HERA-B detector from Novem-

Figure 2. J/ψ signal in J/$\psi \to \mu^+\mu^-$ decays (left) and from J/$\psi \to$ e$^+$e$^-$ decays (right), extracted from minimum bias triggered data.

Figure 3. Transverse momentum distribution d$N/$dp_T^2 of J/$\psi \to$ e$^+$e$^-$ decays.

ber 2002 to February 2003. In dilepton triggered data, about 170,000 J/$\psi \to \mu^+\mu^-$ decays and about 150,000 J/$\psi \to$ e$^+$e$^-$ decays have been reconstructed. In addition, about 200 million events have been recorded with the minimum bias trigger.

4. Charmonium Production

4.1. J/ψ Cross Section

A clean J/ψ signal is observed in the data recorded with the minimum bias trigger. The invariant mass distributions for the dimuon and the dielectron channels are shown in Fig. 2. From these signals the J/ψ production cross section can be extracted without trigger bias.

4.2. J/ψ Differential Distributions

From data recorded with the dilepton trigger, differential cross sections of J/ψ production are determined. As an example, in Fig. 3, the J/$\psi \to$ e$^+$e$^-$ yield for 25% of the full statistics is shown as a function of the transverse momentum p_T. The HERA-B detector covers a broad kinematic range of 0.0 to 4.8 GeV/c. The p_T spectrum is fitted with the parametrization function

$$\frac{\text{d}\sigma}{\text{d}p_T^2} = A \cdot \left[1 + \left(\frac{35\pi p_T}{256 \langle p_T \rangle}\right)^2\right]^{-6}, \tag{1}$$

in which the normalization constant A and the average transverse momentum $\langle p_T \rangle$ are free parameters. In Table 1, preliminary HERA-B results on $\langle p_T \rangle$ are shown. The comparison of different target materials and with results of the experiments E771 [1] and E789 [2] shows an increase of $\langle p_T \rangle$ with the atomic mass number.
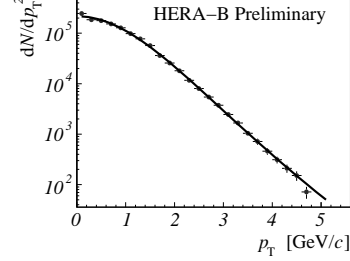
4.3. A-Dependence of J/ψ Production

Nuclear effects in heavy quark production are commonly parametrized by the power law

$$\sigma_{\text{p}A} = \sigma_{\text{p}N} \cdot A^{\alpha(x_\text{F}, p_\text{T})}. \tag{2}$$

Here, $\sigma_{\text{p}A}$ is the proton-nucleus cross section, $\sigma_{\text{p}N}$ is the proton-nucleon cross section, and A is the atomic mass number of the target. A value of $\alpha(x_\text{F}, p_\text{T}) < 1$ corresponds to suppression of heavy quark production. The sources of nuclear suppression in J/ψ production are either interactions of the partons in the initial state with the nuclear medium, or the absorption of the c$\bar{\text{c}}$ pre-state or the final J/ψ, see e.g. [3].

In HERA-B, the suppression parameter α is extracted from data samples taken with a carbon and a tungsten target simultaneously. This setup is utilized to minimize systematic uncertainties in the detector and trigger performance. Using $\sigma = N/(\mathscr{L}\varepsilon)$, Eq. (2) can be solved for α:

$$\alpha = \frac{1}{\log(A_\text{W}/A_\text{C})} \cdot \log\left(\frac{N_\text{W}}{N_\text{C}} \cdot \frac{\mathscr{L}_\text{C}}{\mathscr{L}_\text{W}} \cdot \frac{\varepsilon_\text{C}}{\varepsilon_\text{W}}\right). \tag{3}$$

The A-dependence measurement hence includes measuring three ratios, the ratio of J/ψ yields, N_W/N_C, the ratio of luminosities per wire, $\mathscr{L}_\text{C}/\mathscr{L}_\text{W}$, and the ratio of efficiencies, $\varepsilon_\text{C}/\varepsilon_\text{W}$. The luminosity ratio is extracted from the number of interactions in minimum bias events recorded in parallel to the triggered data. The ratio of efficiencies is determined from a detailed Monte Carlo (MC) simulation of the HERA-B detector and trigger. Preliminary results on $\alpha(x_\text{F})$, based on 10% of the full statistics, are presented in Fig. 4. Data from different combinations of carbon and tungsten wires show results consistent with the previous result by the E866 collaboration [4]

Table 1
HERA-B preliminary results on the average transverse momentum $\langle p_T \rangle$ for $J/\psi \to e^+e^-$ and $J/\psi \to \mu^+\mu^-$ decays, compared to results of previous experiments.

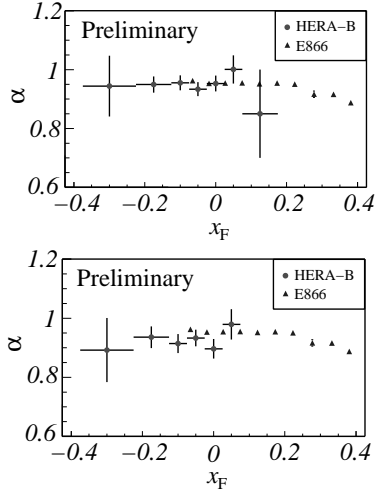| Target	Experiment	Max. p_T	$\langle p_T \rangle$[GeV/c](e^+e^-)	$\langle p_T \rangle$[GeV/c]($\mu^+\mu^-$)
C, 920 GeV	HERA-B Preliminary	4.8 GeV/c	1.22 ± 0.01(stat.)	1.22 ± 0.01(stat.)
W, 920 GeV	HERA-B Preliminary	4.8 GeV/c	1.29 ± 0.01(stat.)	$1,30 \pm 0.01$(stat.)
Si, 800 GeV	E771 [1]	3.5 GeV/c		1.20 ± 0.01
Au, 800 GeV	E789 [2]	2.6 GeV/c		1.290 ± 0.009

Figure 4. Nuclear suppression parameter $\alpha(x_F)$ for two different combinations of carbon and tungsten wires, compared to the result of E866 [4].
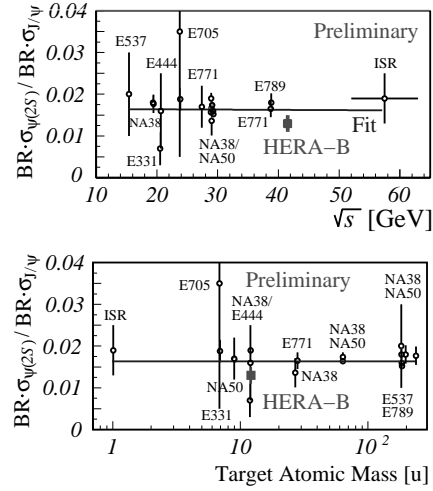

Figure 5. $\psi(2S)$-to-J/ψ production ratio as a function of the center-of-mass energy $\sqrt{s}$ (top) and the atomic mass number A (bottom). The preliminary HERA-B result (square) is compared to results of previous experiments.

in the overlap region and allow the measurement to be extended to $x_F = -0.3$.

4.4. $\psi(2S)$ Production

The production cross section for $\psi(2S)$ mesons is measured relative to the J/ψ cross section in order to reduce systematic uncertainties. In order to extract

$$R = \frac{\mathrm{BR}(\psi(2S) \to \ell^+\ell^-) \cdot \sigma_{\psi(2S)}}{\mathrm{BR}(J/\psi \to \ell^+\ell^-) \cdot \sigma_{J/\psi}} = \frac{N_{\psi(2S)}}{N_{J/\psi}} \cdot \frac{\varepsilon_{J/\psi}}{\varepsilon_{\psi(2S)}}, \tag{4}$$

the relative yield $N_{\psi(2S)}/N_{J/\psi}$ is corrected by the efficiency ratio $\varepsilon_{J/\psi}/\varepsilon_{\psi(2S)}$, which is obtained from a MC simulation.

A preliminary result for the e^+e^- channel is $R = 0.13 \pm 0.02$(stat.). As shown in Fig. 5, this result

agrees well with previous measurements, both as a function of the center-of-mass energy and the atomic mass number.

4.5. χ_c Production

The fraction of J/ψ produced via the radiative decay $\chi_{c1,2} \to J/\psi \gamma \to \mu^+\mu^-\gamma$,

$$R(\chi_c) = \frac{\sum_{J=1}^{2} \sigma_{\chi_{cJ}} \cdot \mathrm{BR}(\chi_{cJ} \to J/\psi\gamma)}{\sigma_{J/\psi}} = \frac{N_{\chi_c}}{N_{J/\psi}} \cdot \frac{\varepsilon_{J/\psi}}{\varepsilon_{\chi_c} \cdot \varepsilon_\gamma}, \tag{5}$$

provides a good test of charmonium production models. As depicted in Fig. 6, the χ_c signal is extracted from the mass difference distribution of the $\mu^+\mu^-\gamma$
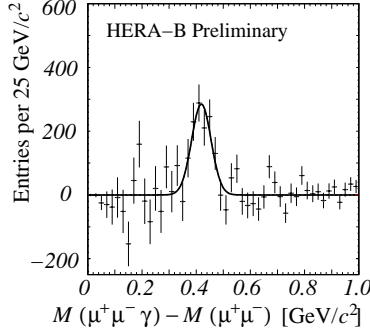
Figure 6. χ_c signal in mass difference distribution $M(\mu^+\mu^-\gamma) - M(\mu^+\mu^-)$. Combinatorial background has been subtracted.

and the $\mu^+\mu^-$ systems. The efficiency ε_γ to detect the additional photon is determined from a MC simulation.

A preliminary analysis of a part of the 2002/2003 data yields $R(\chi_c) = 0.21 \pm 0.5$(stat.). This result is consistent with the previous HERA-B result, $R(\chi_c) = 0.32 \pm 0.6$(stat.) ± 0.4(syst.) [5].

5. Open Charm Production

5.1. D Meson Production Cross Sections

D meson production is studied using minimum bias triggered data. The signals shown in Fig. 7 are obtained imposing cuts on the separation of the decay vertex from the primary vertex and the impact parameter to the target wire.

Using these data, the production cross section for D^0 and D^+, $\sigma_{D^0|D^+} \equiv (\sigma_{D^0} + \sigma_{D^+})/2$, is determined, and the production ratios $\sigma_{D^+}/\sigma_{D^0}$ and $\sigma_{D^{*+}}/\sigma_{D^0}$ are extracted. The cross sections obtained in the limited acceptance of the HERA-B detector are extrapolated to the full x_F range using Pythia. Preliminary results of these measurements are summarized in Table 2. As shown in Fig. 8, the result on $\sigma_{D^0|D^+}$ agrees well with other measurements at similar beam energies. The HERA-B measurement of the ratio $\sigma_{D^+}/\sigma_{D^0}$ is in good agreement with pion-induced results at lower center-of-mass energies. HERA-B will improve the results of previous proton-induced experiments at similar energies.
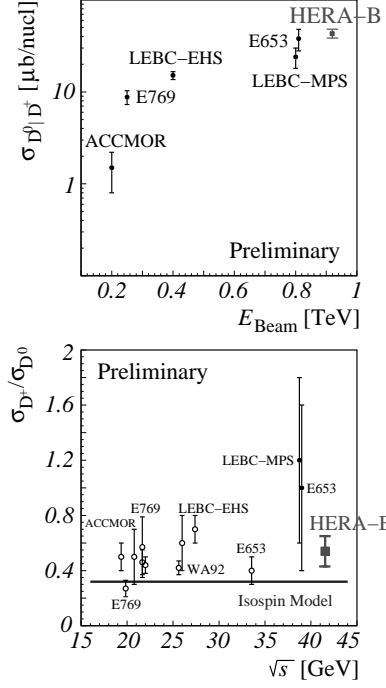

Figure 8. D^0 and D^+ production cross sections (top) and cross section ratio (bottom), compared to results of previous experiments. Pion-induced results are depicted as open circles, while closed circles stand for proton-induced results. The line indicates a prediction for the production ratio based on an isospin model [6].

5.2. Limit on $D^0 \to \mu^+\mu^-$

An upper limit on the branching fraction of the flavor-changing neutral current process $D^0 \to \mu^+\mu^-$ has been determined analyzing data collected with the dimuon trigger. As shown in Fig. 9, three events are observed in the signal region, while the expected background amounts to 6.0 ± 1.2 events. From these numbers, an upper limit for the $D^0 \to \mu^+\mu^-$ branching fraction of 2.0×10^{-6} is obtained at 90% confidence level [7].

6. Summary

Measuring the properties of open and hidden charm production in proton-nucleus interactions is one of the main physics goals of the HERA-B experiment. This paper presents preliminary results on a variety of physics studies, including open charm and charmo-
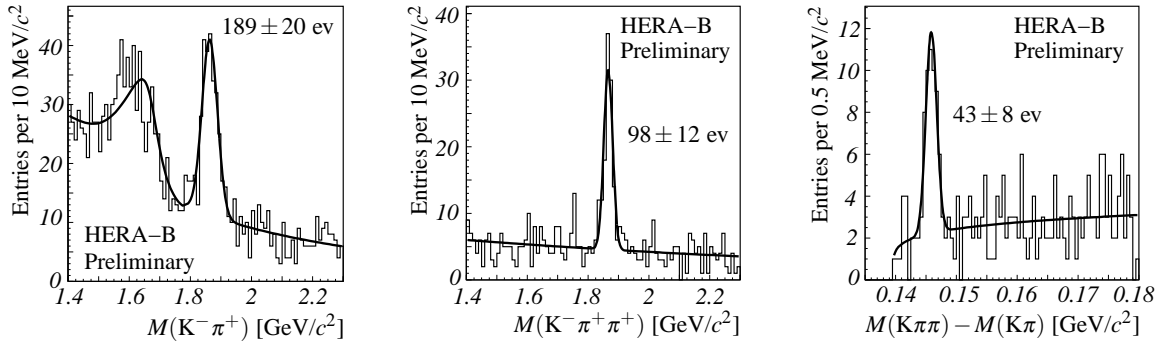
Figure 7. Open charm decays observed in the minimum bias data-set: $D^0 \to K^-\pi^+$ (left), $D^+ \to K^+\pi^+\pi^-$ (middle), and $D^{*+} \to D^0\pi^+ \to K^-\pi^+\pi^+$ (right). The corresponding charge-conjugated channels are included.

Table 2
Production cross sections and cross section ratios for D^0, D^+, and D^{*+} decays. The cross sections are given with statistical and systematic uncertainties.

Preliminary	$-0.1 < x_F < 0.05$	Full x_F range
σ_{D^0} [μb/nucl]	$21.4 \pm 3.2 \pm 3.6$	$56.3 \pm 8.5 \pm 9.5$
σ_{D^+} [μb/nucl]	$11.5 \pm 1.7 \pm 2.2$	$30.2 \pm 4.5 \pm 5.8$
$\sigma_{D^{*+}}$ [μb/nucl]	$10.0 \pm 1.9 \pm 1.4$	$27.8 \pm 5.2 \pm 3.9$
$\sigma_{D^+}/\sigma_{D^0}$		$0.54 \pm 0.11 \pm 0.14$
$\sigma_{D^{*+}}/\sigma_{D^0}$		$0.54 \pm 0.12 \pm 0.10$

nium production cross sections in proton-nucleus collusions, differential distributions and nuclear effects. The HERA-B collaboration is looking forward to finalizing these promising analysis efforts in the near future.
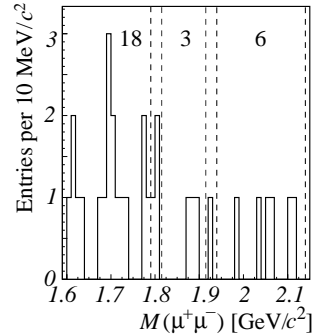
7. Acknowledgements

Figure 9. Dimuon invariant mass spectrum in the D^0 region. The numbers of events in the signal region (middle) and sideband regions are given [7].

REFERENCES

1. T. Alexopoulos et al., Differential cross sections of J/ψ and ψ' in 800-GeV/c p-Si interactions, Phys. Rev. D55 (1997) 3927–3932.

2. M. H. Schub et al., Measurement of J/ψ and ψ' production in 800-GeV/c proton-gold collisions, Phys. Rev. D52 (1995) 1307–1315.

3. R. Vogt, The x_F dependence of ψ and Drell-Yan production, Phys. Rev. C61 (2000) 035203.

4. M. J. Leitch et al., Measurement of J/ψ and ψ' suppression in pA collisions at 800-GeV/c, Phys. Rev. Lett. 84 (2000) 3256–3260.

5. I. Abt et al., J/ψ production via χ_c decays in 920 GeV pA interactions, Phys. Lett. B561 (2003) 61–72.

6. S. Frixione, M. L. Mangano, P. Nason, G. Ridolfi, Heavy-quark production, Adv. Ser. Direct. High Energy Phys. 15 (1998) 609–706.

7. I. Abt et al., Search for the flavor-changing neutral current decay $D^0 \to \mu^+\mu^-$ with the HERA-B detector, Phys. Lett. B596 (2004) 173–183.